RESEARCH ARTICLE

Hippocampal Pathology in the Human Neuronal Ceroid-Lipofuscinoses: Distinct Patterns of Storage Deposition, Neurodegeneration and Glial Activation

Jaana Tyynelä[1,2]: Jonathan D Cooper[3,5,6]; M Nadeem Khan[4,5]; Stephen JA Shemilt[3,5,6]; Matti Haltia[2]

[1] Institute of Biomedicine/Biochemistry and Neuroscience Research Program and [2]Department of Pathology, University of Helsinki, Finland.
[3] Pediatric Storage Disorders Laboratory and [4]MRC London Neurodegenerative Diseases Brain Bank, [5]Departments of Neuropathology and [6]Neuroscience, Institute of Psychiatry, King's College, London, United Kingdom.

Corresponding author:
Jaana Tyynelä, Institute of Biomedicine/Biochemistry, PO Box 63 (Haartmanink. 8), FIN-00014 University of Helsinki, Finland (E-mail: jaana.tyynela@helsinki.fi)

The neuronal ceroid-lipofuscinoses (NCLs) are recessively inherited lysosomal storage diseases, currently classified into 8 forms (CLN1-CLN8). Collectively, the NCLs constitute the most common group of progressive encephalopathies of childhood, and present with visual impairment, psychomotor deterioration and severe seizures. Despite recent identification of the underlying disease genes, the mechanisms leading to neurodegeneration and epilepsy in the NCLs remain poorly understood. To investigate these events, we examined the patterns of storage deposition, neurodegeneration, and glial activation in the hippocampus of patients with CLN1, CLN2, CLN3, CLN5 and CLN8 using histochemistry and immunohistochemistry. These different forms of NCL shared distinct patterns of neuronal degeneration in the hippocampus, with heavy involvement of sectors CA2-CA4 but relative sparing of CA1. This selective pattern of degeneration was also observed in immunohistochemically identified interneurons, which exhibited a graded severity of loss according to phenotype, with calretinin-positive interneurons relatively spared. Furthermore, glial activation was also regionally specific, with microglial activation most pronounced in areas of greatest neuronal loss, and astrocyte activation prominent in areas where neuronal loss was less evident. In conclusion, the NCLs share a common pattern of selective hippocampal pathology, distinct from that seen in the majority of temporal lobe epilepsies.

Brain Pathol 2004;14:349-357.

INTRODUCTION

The neuronal ceroid-lipofuscinoses (NCLs) are a genetically and clinically heterogeneous group of at least 8 fatal childhood brain disorders (9, 15, 19, 20, 28, 29). The NCLs typically show an autosomal recessive pattern of inheritance with an estimated global incidence of 7 to 8 per 100 000 live births (20, 29). Two early-onset clinical types, CLN1 and CLN2, are marked by deficiencies of the lysosomal enzymes palmitoyl-protein thioesterase 1 (PPT1; 39) and tripeptidyl peptidase I (TPPI; 37), respectively. PPT1 is a 35 to 37 kDa glycoprotein, which removes fatty acids from various acylated proteins and peptides in vitro (2, 6, 10). In the central nervous system (CNS), PPT1 has recently been found to localize to synaptic vesicles (23, 38) and to be trafficked to axons (1, 35). PPT1 knock-out mice exhibit an NCL-like neurologic phenotype and neuropathologic markers typical of NCL (3, 16). TPPI is a pepstatin-insensitive lysosomal serine protease, cleaving the N-terminal tripeptides from peptides and small proteins (41, 42), and may have a nonredundant role in the brains (43). In contrast, 4 other types of NCL (CLN3, CLN5, CLN6, and CLN8) are marked by mutations in genes encoding novel proteins (14, 21, 33, 36, 44). The physiological functions of these proteins remain to be elucidated (22, 24, 25, 40).

Despite this genetic heterogeneity, the NCLs share a relatively uniform neuropathologic phenotype, characterized by widespread intracellular accumulation of ceroid- and lipofuscin-like proteinaceous material (9, 19, 20). All forms of NCLs are further characterized by selective and progressive neuronal loss within the CNS and usually also in the retina (19, 20, 27). The extent of neurodegeneration is most severe in the early-onset forms of NCL, including infantile onset CLN1 and late-infantile onset CLN2, in which there are few surviving neurons in the neocortex at the time of autopsy (15, 17, 18, 19).

The main clinical characteristics of the NCLs are mental deterioration, visual impairment (except in CLN4 and CLN8), loss of motor skills, and epilepsy. Indeed, epileptic seizures are a main symptom in all forms of NCL and the leading sign in CLN2, and CLN8 (19, 20). These seizures may be partial or complex and may be controlled by a combination of drugs, with varied efficacy across different forms of NCL (Åberg, Santavuori, Vanhanen, personal communication). The pathogenesis of epilepsy in the NCLs remains largely unknown although the loss of interneurons observed in murine models of NCL may contribute to this phenotype (3, 8, 9, 26). At the terminal stage, the hippocampus is almost completely destroyed in CLN1 (17, 18), but very little information is available for other forms of NCL. The aim of this study was to analyze hippocampal pathology in different forms of NCL, as an initial step towards understanding the mechanisms that underlie neuronal death and seizure generation.

MATERIALS AND METHODS

Tissue specimens. Paraffin-embedded tissue samples were obtained from the archives of Helsinki University Department of Pathology and the MRC London Neurodegenerative Diseases Brain Bank. These specimens were obtained at routine autopsies of NCL patients or age-matched controls with informed written consent from their families. At autopsy, tissues

NEURONAL LOSS						
	SUB	CA1	CA2	CA3	CA4	DG
CLN1 (n = 1)[1]	1-2	3-4	4	4	3	3
CLN1 (n = 2)[2]	3-4	4	4	4	4	4
CLN2 (n = 1)[3]	3-4	4	4	4	4	4
CLN3 (n = 4)[4]	0	0-1	2-3	3-4	2-3	0-1
CLN5 (n = 1)[5]	1	1	2	1	1	0
CLN5 (n = 1)[6]	0-1	1	3	4	4	3-4
CLN8 (n = 2)[7]	0	0	1-3	0-1	0-1	0
CLN8 (n = 1)[8]	0	0	3-4	1	1	0

[1] Early stage pathology, death at 5 years; [2]advanced pathology, death at 10 and 11 years; [3]advanced pathology, death at 26 years; [4]advanced pathology, death at 16, 19, 23, and 28 years; [5]early stage pathology, death at 15 years; [6]advanced pathology, death at 22 years; [7]early stage pathology, death at 23 and 38 years; [8]advanced pathology, death at 60 years.

Table 1.

NEURONAL STORAGE						
	SUB	CA1	CA2	CA3	CA4	DG
CLN1 (n = 1)[1]	3	2	-	-	4	3
CLN1 (n = 2)[2]	-	-	-	-	-	-
CLN2 (n = 1)[3]	-	-	-	-	-	-
CLN3 (n = 4)[4]	1-2	1-2	3-4	2-3	2-3	1-2
CLN5 (n = 1)[5]	2-3	1	4	3	3	2
CLN5 (n = 1)[6]	3	1	4	-	-	2
CLN8 (n = 2)[7]	0-3	0-1	3-4	1-3	1-3	1-2
CLN8 (n = 1)[8]	1-3	0-1	3	3	2	2

[1]Early stage pathology, death at 5 years; [2]advanced pathology, death at 10 and 11 years; [3]advanced pathology, death at 26 years; [4]advanced pathology, death at 16, 19, 23, and 28 years; [5]early stage pathology, death at 15 years; [6]advanced pathology, death at 22 years; [7]early stage pathology, death at 23 and 38 years; [8]advanced pathology, death at 60 years

- in areas with total neuronal loss the storage in neurons could not be determined

Table 2.

MICROGLIAL ACTIVATION						
	SUB	CA1	CA2	CA3	CA4	DG
CLN1 (n = 1)[1]	2	3	4	4	4	4
CLN1 (n = 2)[2]	1	1	1	1	1	1
CLN2 (n = 1)[3]	1-2	2	1	1	1	1
CLN3 (n = 4)[4]	1	1-2	2-3	2-3	2-3	1-2
CLN5 (n = 1)[5]	1	1	2	2	1	0
CLN5 (n = 1)[6]	0-1	1	1	2	1	2
CLN8 (n = 2)[7]	1-2	0-1	2	3	2	2
CLN8 (n = 1)[8]	0-1	0	2	1	1	0

[1]Early stage pathology, death at 5 years; [2]advanced pathology, death at 10 and 11 years; [3]advanced pathology, death at 26 years, [4]advanced pathology, death at 16, 19, 23, and 28 years; [5]early stage pathology, death at 15 years, [6]advanced pathology, death at 22 years; [7]early stage pathology, death at 23 and 38 years, [8]advanced pathology, death at 60 years

Table 3.

were fixed immediately by immersion in 4% neutral buffered formaldehyde and subsequently processed and embedded in paraffin. We analyzed autopsy specimens of the temporal lobe of NCL patients with CLN1 (n = 3; ages at death 5, 10, and 11 years), CLN2 (n = 1; age 26 years), CLN3 (n = 4; ages 16, 19, 23, and 28 years), CLN5 (n = 2; ages 15, and 22 years), and CLN8 (n = 3; ages 23 [accidental death], 38, and 60 years); controls (n = 3; ages 2, 25, and 26 years). This study was approved by the Ethical Research Committee of the Institute of Psychiatry (approval numbers 223/00, 181/02).

Histological and histochemical methods. To reveal neuronal morphology and stain for pathological markers associated with NCL, adjacent 4-µm paraffin sections from each case were dewaxed and stained with hematoxylin and eosin, Luxol Fast Blue-cresyl violet, periodic acid Schiff and Sudan Black B methods using standard protocols. The extent of neuronal loss in each hippocampal subfield and the subiculum was scored in a semi-quantitative manner ranging from 0 (no cell loss) to 4 (total cell loss) (Table 1).

Confocal microscopy. Confocal microscopy was used to demonstrate the distribution of autofluorescent storage material in each case. Briefly, 4-µm paraffin sections were dewaxed, rehydrated through a graded series of ethanols, rinsed in TBS (0.05M Tris, 0.15M NaCl, pH = 7.6), and coverslipped using Vectashield (Vector Laboratories, Peterborough, United Kingdom). Subsequently, the extent of autofluorescent storage material was revealed by single channel confocal microscopy (Zeiss LSM 5 Pascal, Carl Zeiss Ltd, United Kingdom) using the 488-nm laser line, maintaining a consistent relative relationship between detector gain and amplitude offset between samples. The extent of storage material accumulation in each hippocampal subfield and the subiculum was scored semi-quantitatively ranging from 0 (no accumulation) to 4 (remaining cells extremely distended with accumulated storage material) (Table 2).

Immunohistochemical staining for markers of glial and interneuron phenotype. A series of adjacent 4-µm paraffin sections from each case were immunohistochemically stained for markers of astrocytosis (GFAP), microglial activation (CD68), and for calcium binding proteins that mark different subpopulations of interneurons, essentially as described (8). Sections were dewaxed in xylene and pretreated either with 0.5% trypsin at 37°C for 40 minutes (GFAP staining), or with 4% (w/v) pepsin in 1% (v/v) HCl at 37°C for 20 minutes (CD68) or processed with no pre-treatment (interneuron markers). All sections were subsequently rinsed in PBS (glial mark-

ers) or TBS (interneuron markers), and endogenous peroxidase activity blocked by incubating the sections in methanol containing 1.6 % hydrogen peroxide at room temperature (RT) for 30 minutes. Sections were then rinsed and blocked in 15% normal serum (NS) (normal goat serum for GFAP; normal horse serum for CD68; normal swine serum and 0.3% Triton X-100 for interneuron markers) at RT for 30 minutes, before overnight incubation at 4°C with primary antiserum diluted in buffer containing 10% NS (polyclonal rabbit anti-GFAP, 1:10,000 and monoclonal mouse anti-CD68, clone PG-M1, 1:800, both from Dako; rabbit anti-parvalbumin, 1:1000; anti-calbindin 1:5,000, anti-calretinin, 1:2,500 from Swant, Bellinzona, Switzerland). Pre-immune serum or buffer was used instead of primary antibodies to verify the specificity of each antiserum. Immunostaining was continued using the appropriate rabbit, mouse or swine Vectastain Elite ABC kit (components diluted at 1:200; Vector Laboratories, Peterborough, United Kingdom), and immunoreactivity was visualized using either 3-amino-9-ethylcarbazole (GFAP and CD68) or diaminobenzidine tetrahydrochloride (interneuron markers) and hydrogen peroxide and counterstained with hematoxylin.

The extent of glial activation in each hippocampal subfield and the subiculum was scored semi-quantitatively ranging from 0 (no activation) to 4 (extreme activation) (CD68 Table 3; GFAP Table 4), as was the loss of interneurons, scored from 0 (no interneuron loss) to 4 (total loss of interneurons) (Table 5).

RESULTS

The overall pattern of neuronal loss demonstrated subfield-specific changes and a spectrum of severity in different forms of NCL. In the early-onset forms of NCL, CLN1 and CLN2, the extreme neuronal loss lead to a complete breakdown of the normal hippocampal architecture as compared to age-matched controls (Table 1). Luxol Fast Blue staining revealed the remnants of the hippocampal formation, which could only be recognized by a dense band of remaining glial cells (Figure 1). In these cases, profound neurodegeneration also extended into the adjacent subiculum and neighboring cortical regions of the temporal lobe. In CLN3, CLN5 and CLN8 cases, the hippocampal formation was better preserved showing a distinct pattern of neuronal loss within different subfields (Figure 1; Table 1). There was also less neuronal loss in the subiculum of these later onset cases, compared to the extent of cell loss in the hippocampal formation. In CLN3 cases, neurodegeneration was most pronounced in the hilus and became progressively less severe moving through CA3 and CA2 with relative sparing of CA1 (Figure 1). This pattern of neurodegeneration was less evident in CLN5 and entirely absent in CLN8 where a unique pattern of regional neuronal loss involving CA2 was present (Figure 1). As in the less advanced case of CLN1 and all CLN3 cases, CA1 was relatively well preserved in both CLN5 and CLN8 cases (Table 1).

Similarly, the degree of neuronal storage varied in different subfields of the hippocampus of NCL cases (Table 2), as visualized by Luxol Fast Blue staining (Figure 1) or confocal microscopy (Figure 2). The appropriately aged control cases exhibited minimal storage material in all regions of the hippocampus, as would be expected (Figure 1). In CLN1 and CLN2 cases, it was not possible to estimate the degree of storage in neurons because of the complete neuronal loss, except in one CLN1 case (age at death 5 years), which represented an earlier stage of the degenerative process. In this less advanced CLN1 case, the remaining neurons were profoundly ballooned with only very few thickened processes visible (Figure 2). In CLN3, CLN5 and CLN8, storage was most pronounced in neurons and macrophages within CA2, and marked in CA3 and CA4 (Figure 2). In certain cases, moderate storage was also observed in the small granular neurons of the dentate gyrus, resulting in an elongation of their soma (Figure 2). There was comparatively little storage in the neurons of CA1 in all forms of NCL (Figure 2), while

ASTROCYTIC ACTIVATION						
	SUB	CA1	CA2	CA3	CA4	DG
CLN1 (n = 1)[1]	3	3	4	3	3	2
CLN1 (n = 2)[2]	2	2	2-3	2-3	1	2
CLN2 (n = 1)[3]	2-3	1	1	1	2	3
CLN3 (n = 4)[4]	1-2	2	2-3	2-3	2	1
CLN5 (n = 1)[5]	2	1	3	2	2	1
CLN5 (n = 1)[6]	2-3	2	2	1	1	2
CLN8 (n = 2)[7]	2	0	0-3	1-2	1-3	0-2
CLN8 (n = 1)[8]	2	1†	2	2	2	1†

[1]early stage pathology, death at 5 years; [2]advanced pathology, death at 10 and 11 years; [3]advanced pathology, death at 26 years; [4]advanced pathology, death at 16, 19, 23, and 28 years; [5]early stage pathology, death at 15 years; [6]advanced pathology, death at 22 years; [7]early stage pathology, death at 23 and 38 years; [8]advanced pathology, death at 60 years; †pronounced activation was found in stratum oriens adjacent to CA1 principal neurons and adjacent to the granular neurons of DG.

Table 4.

INTERNEURON LOSS PV, Cb, CR						
	SUB	CA1	CA2	CA3	CA4	DG
CLN1 (n=1)[1]	3, 3, 3	4, 3, 3	4, 4, 3	4, 4, 4	-, -, -	4, -, -
CLN1 (n=1)[2]	4, 3, 3	4, 4, 4	4, 4, 4	4, 4, 4	-, -, -	4, -, -
CLN2 (n=1)[3]	4, 3, 3	4, 4, 4	4, 4, 4	4, 4, 4	-, -, -	4, -, -
CLN3 (n=3)[4]	1, 0, 0	2, 1, 1	3, 3, 2	2, 3, 2	-, -, -	2, -, -
CLN5 (n=1)[5]	2, 3, 2	2, 3, 3	4, 4, 4	3, 4, 4	-, -, -	3, -, -
CLN5 (n=1)[6]	3, 3, 3	3, 3, 3	4, 4, 4	4, 4, 4	-, -, -	4, -, -
CLN8 (n=1)[7]	1, 1, 1	2, 2, 1	4, 4, 4	3, 2, 2	-, -, -	3, -, -

[1]early stage pathology, death at 5 years; [2]advanced pathology, death at 10 and 11 years; [3]advanced pathology, death at 26 years, [4]advanced pathology, death at 19, 23, and 28y; [5]early stage pathology, death at 15y, [6]advanced pathology, death at 22y; [7]early stage pathology, death at 38y; - indicates antigen not expressed in interneurons in this sub-field

Table 5.

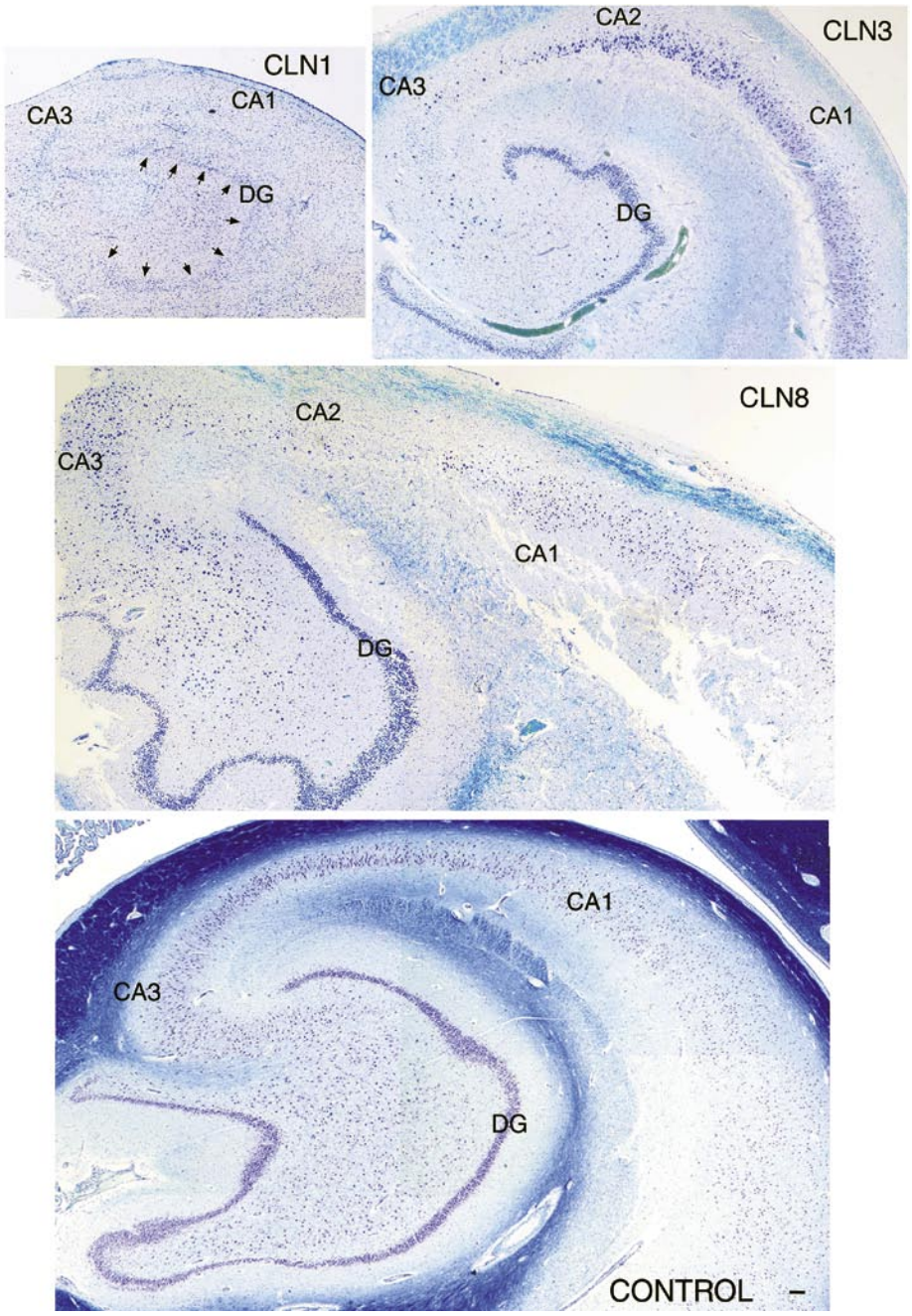

Figure 1. Neuronal loss in the NCL hippocampus. Luxol Fast Blue—cresyl violet staining revealed specific patterns of neuronal loss and storage deposition in different forms of NCL. The normal hippocampal architecture displayed by control cases was completely disrupted in pathologically advanced cases of CLN1, with only a dense band of glial scaring (arrows) remaining to mark the position of the dentate gyrus (DG). In contrast, hippocampal subfields showed different degrees of degeneration in CLN3 cases, with the hilus and CA3 exhibiting most profound loss of neurons and with relative preservation of CA1. CLN8 cases exhibited a characteristic selective degeneration of neurons in CA2, with relative preservation of other subfields. Scale bar = 100 μm.

the build-up of storage material was quite pronounced in the entorhinal cortex and subiculum. In the subiculum, the distribution of storage material was not uniform, being largely confined to the deeper layers (data not shown).

To map regional differences in microglial activation, we stained each case for the macrophage marker CD68 (Table 3). In cases of CLN1 and CLN2 where neuronal loss was most pronounced, the macrophage response had already subsided with very few CD68 immunoreactive microglia present. In contrast, in a less advanced case of CLN1 where neuronal loss was still in progress, CD68-positive microglia were abundant but to varying degrees in each hippocampal subfield. Comparing patients with CLN1 and CLN5 at different ages, the macrophage reaction was most severe in CA2 in younger patients but became more pronounced in CA3 and CA4 with increasing age, suggesting that neuronal death may initially occur in CA2 and sequentially spread towards CA3 and CA4. There was relatively little variation in the pathological profiles of the four CLN3 cases. In these cases, CD68 staining was most pronounced in CA3, which showed the greatest ongoing neuronal loss, and least evident in CA1 where neurons were better preserved (Figure 3). CD68 immunoreactive microglia exhibited a range of morphologies, but were most often spherical or macrophage-like and found in clusters. Microglial activation in CLN5 and CLN8 cases reflected the relative degree of regional neuronal loss (Table 3). In CLN8, a number of CD68-positive cells were observed in the vicinity of CA2, which exhibited the most severe neuronal death. However, this correlation between neuronal loss and microglial activation was not maintained in all subfields. For example, in CLN3 and one CLN8 case, pronounced microglial activation was present in the dentate gyrus with no obvious neuronal loss (Figure 3). Control tissue typically exhibited very little CD68 immunoreactivity with only occasional CD68 positive microglia present within the hippocampus (data not shown).

Immunohistochemical staining for GFAP revealed that subfield-specific changes also existed for astrocytic activation across all forms of NCL (Table 4; Figure 3). In addition to areas with on-going neuronal loss, hypertrophic astrocytes were observed in areas where neuronal loss was least evident. For example, CA1 which showed most neuronal preservation also showed most pronounced astrocyte hypertrophy. Adjacent to CA1, differences in the extent of astrocyte activation were also observed, with the stratum oriens containing more GFAP-positive cells than the stratum radiatum. An intense band of GFAP-positive astrocytes was often present in the hilar formation, immediately adjacent to the dentate gyrus, which itself showed a variable degree of astrocytosis. In one case of CLN5 where severe ballooning of the surviving CA2 neurons was evident, the neuronal soma appeared encircled by

GFAP immunoreactive processes (Figure 4). Indeed, with the exception of CLN1 and CLN2 cases, GFAP-positive processes were often found in close apposition to surviving neurons (Figure 4). GFAP-positive astrocytes present in the hippocampus of control cases exhibited no signs of hypertrophy or hyperplasia.

To survey changes in the survival of populations of GABAergic interneurons, we stained for calcium binding proteins that mark different subpopulations of interneurons (13). Compared with control cases, loss of interneurons was almost complete in cases of CLN1 and CLN2, but persisting interneurons were evident in other forms of NCL (Table 5) (Figure 5). CLN3 cases contained relatively more interneurons positive for each antigen than any other form of NCL (Table 5). Interneurons were more severely affected in CLN5 than CLN8 (Table 5). Subfields that showed most pronounced pyramidal cell loss also exhibited the greatest loss of interneurons, except for CLN3 cases, where the interneuron loss was far less evident across all subfields. Interestingly, loss of GABAergic interneurons was more profound in the stratum oriens than in the stratum radiatum, thus correlating with the relative levels of astrocytic activation in these subfields. Regional effects on interneuron survival were also present in the subiculum and adjacent entorhinal cortex, which showed relatively little loss of interneurons compared to the hippocampal formation across all forms of NCL. Nevertheless, in CLN1 and CLN2, interneuron loss was so severe in the cortex that only few ballooned interneurons could be found.

In all studied NCL cases, persisting interneurons also exhibited a phenotype-specific survival effect, with calretinin-positive interneurons most spared across all regions. Calbindin is also expressed by granular neurons of the dentate gyrus and their fiber projections. These calbindin-positive granule neurons were best preserved in CLN3 and CLN8, but were almost entirely absent in other forms of NCL. Comparison of the morphology of interneurons revealed common themes between the different forms of NCL (Figure 6). Hypertrophy of the soma of interneurons was most pronounced in CLN1 and CLN2 where only few immunoreactive interneurons were present in the hippocampus and adjacent subiculum. In these neurons, the prominent accumulation of storage material often resulted in redistribution of immunoreactive calcium binding proteins. In contrast, in CLN3 cases the hypertrophy of interneurons was not as severe. In CLN5 and CLN8, interneurons showed more morphological variation.

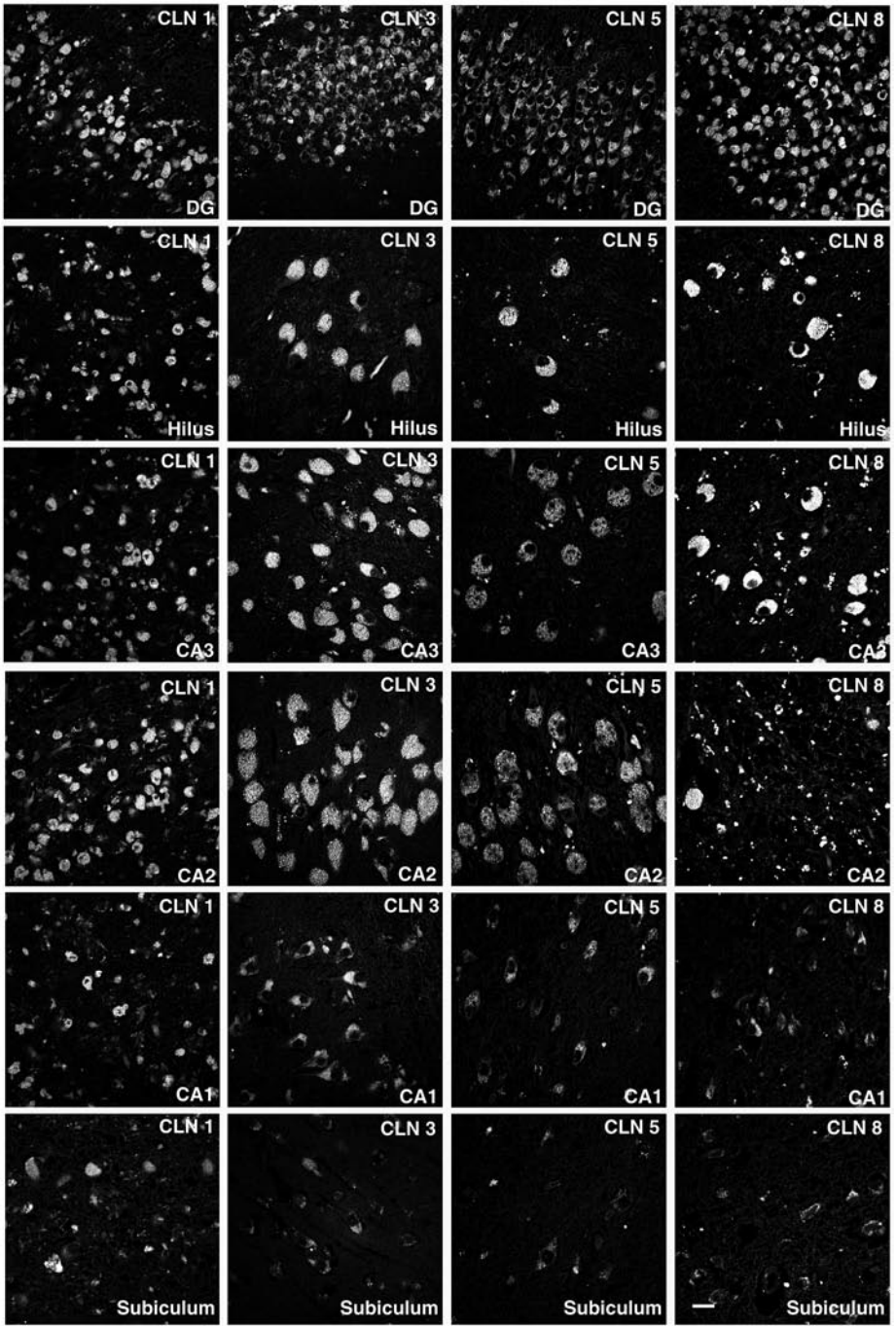

Figure 2. Accumulation of autofluorescent storage material in the NCL hippocampus. Single channel confocal microscope images revealed the extent of storage material accumulation in CLN1, CLN3, CLN5 and CLN8 cases. In a pathologically less advanced CLN1 case, all remaining neurons were filled with storage material. In CLN3 and CLN5 cases, the accumulation of storage material was most pronounced within CA2, and was also marked in CA3 and the hilus compared to the subiculum. This pattern of storage deposition was similar in CLN8 cases, with the exception of CA2 where neuronal loss was essentially complete. There was comparatively little storage material in CA1 neurons in all forms of NCL. DG = dentate gyrus. Scale bar = 20 μm.

DISCUSSION

This systematic survey of neuronal degeneration and glial activation across different forms of NCL has revealed distinct patterns in the degeneration of pyramidal and interneuron populations and the extent of microglial and astrocyte activation

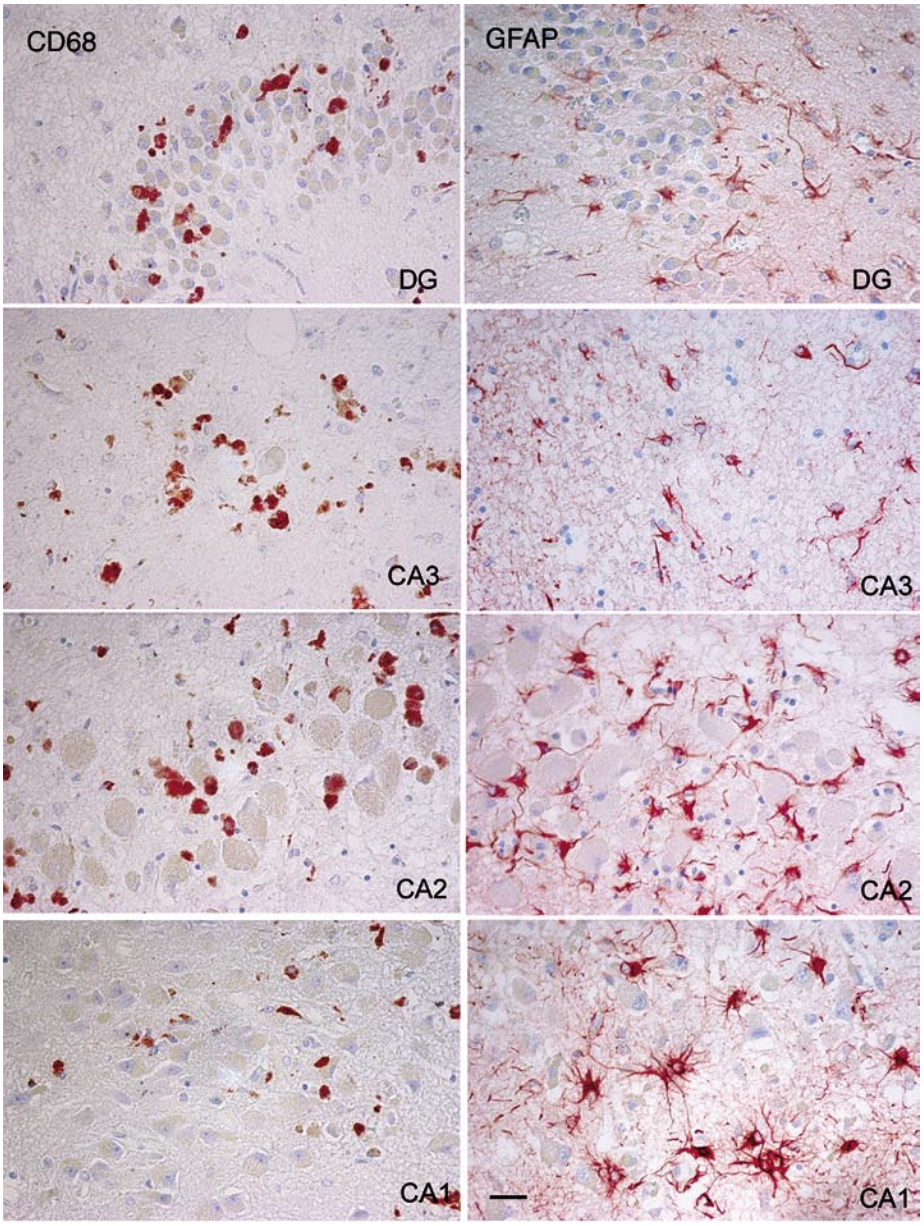

Figure 3. Subfield specific microglial and astrocytic activation in CLN3. Immunohistochemical staining for CD68 revealed that CD68-positive microglia were frequent in the dentate gyrus (DG), CA3 and CA2 hippocampal subfields, where ongoing neuronal loss was most marked. CD68-immunoreactive cells were less frequent in CA1, where neurons were best preserved. In contrast, immunohistochemical staining for GFAP showed that GFAP-positive astrocytes were present in all subfields, but were more frequent in CA1 and CA2. Comparing these regions, astrocyte hypertrophy was particularly prominent in CA1 with enlarged soma and numerous thickened processes. Scale bar = 20 μm.

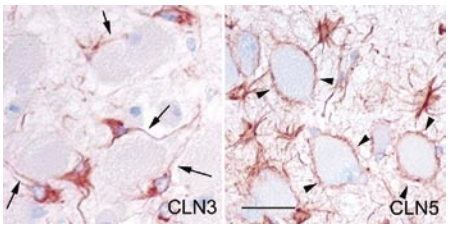

Figure 4. Astrocytic activation and neuron survival in the NCL hippocampus. GFAP-positive processes were frequently found in close apposition to surviving neurons, as shown for neurons in the CA2 hippocampal subfield of a CLN3 case (arrows). In one CLN5 case, GFAP-positive processes completely encircled the persisting neurons in CA2 (arrowheads). Scale bar = 20 μm.

in different hippocampal subfields. Archival material of the type used in this study is of very limited availability, and the small number of cases currently available largely precludes more detailed quantitative analysis. However, systematic semi-quantitative analyses provide invaluable information about pathologic themes across different forms of NCL. With an increasing number of murine and large animal models available for different forms of NCL (9, 27), it will be essential to validate these models by performing comparative analysis with the few post mortem samples that exist from NCL patients.

A consistent finding across all forms of NCL was the relative sparing of both pyramidal neurons and interneurons in CA1 compared to other subfields of the hippocampus. This characteristic pattern is markedly distinct from the pattern of neuron loss seen in the majority of temporal lobe epilepsies (11). As such, this NCL-specific pattern of neuronal loss is unlikely to be a mere consequence of seizure activity but rather reflects a distinctive feature of NCL pathogenesis. The absence of correlation between the extent of storage material accumulation and neuronal loss suggests that storage deposition is not itself directly responsible for neuronal death. Instead, other mechanisms are likely to have significant influence on determining neuronal survival. The marked similarity in the patterns of pyramidal neuron and interneuron loss in each subfield suggests that the balance between excitatory and inhibitory influences is not maintained in the NCLs, as has recently been demonstrated in a mouse model of CLN3 (7). Our findings further emphasize that the balance between these excitatory and inhibitory cell types is potentially of key importance in NCL pathogenesis. Such excitatory/inhibitory imbalance may lead not only to excitatory neuronal death but possibly also to abnormal synaptic circuitry between persisting neuronal populations.

Previous studies of the neocortex of human NCL patients described a loss of small stellate neurons, which were presumed to be GABAergic (4, 5), and a loss of ultrastructurally identified inhibitory synapses (45), suggesting that GABAergic neuronal populations may be severely affected in at least some forms of NCL. It is now evident that interneuron populations are lost in multiple murine and ovine models of NCL (8, 9, 26, 27, 31). However, the present study is the first systematic demonstration that immunohistochemical markers of interneuron phenotype are also affected in human NCL. The relative resistance of calretinin-positive interneurons in multiple forms of NCL is also characteristic of animal models (3, 9), and may reflect their relative resistance to long-term excitotoxic

stress. Indeed, the relative resistance of calretinin- versus parvalbumin- and calbindin- positive interneurons has recently been reported in vitro (12).

The regional differences in neuronal loss were accompanied by regionally selective microglial activation in different hippocampal subfields in all forms of NCL, a feature that is also evident in a mouse model of CLN1 (3). Microglial activation correlated with on-going neuronal loss across all cases of NCL examined, being most prominent during early stages of neurodegeneration and then subsiding once neuronal loss is complete, as with the pathologically advanced cases of CLN1 and CLN2. The absence of prolonged microglial activation in these cases may represent an NCL-specific mechanism in which these cells are themselves targeted as part of the disease process. These temporal and regional changes may reflect differential expression of cytokines or other signalling molecules that influence microglial activation and/or recruitment (34).

In many neurodegenerative conditions reactive astrocytosis often accompanies neuronal loss and serves as an early indicator of damage within affected areas. As such, the mechanisms controlling astrocytosis in areas, where neuronal degeneration is not evident remain to be elucidated. For example, astrocytic activation was often pronounced in the stratum oriens immediately adjacent to CA1, and also extended into this cell layer. Astrocytes not only play an important role in controlling the microenvironment surrounding neurons, but also directly influence neuronal activity (30, 32). Importantly, the degree of astrocyte coverage is important for the clearance of glutamate, thereby controlling the extracellular glutamate concentration (30). In this context, the observation of GFAP immunoreactive processes completely encircling or in close apposition to ballooned neurons may represent a protective astrocytic response to excitatory imbalances in NCL. Indeed, this feature of astrocytosis may be unique to the NCLs as we have not seen this phenomenon in a range of other storage diseases, including GM1 and GM2 gangliosidoses, Nieman-Pick C and Gaucher diseases, Arylsulfatase deficiency, and different forms of MPS.

The interplay of cellular responses in the NCLs produces a characteristic neuropathological profile that is distinct from classical temporal lobe epilepsies. This specific pattern of neuronal loss may reflect cellular connectivity or individual neuronal vulnerability to molecular events that are, as yet, unidentified. In this respect, it is interesting to note that the pathologic changes in CLN1, CLN2 and CLN5, caused by defects in soluble proteins, are more severe than those in CLN3 and CLN8 which are caused by defects in transmembrane proteins. These findings are consistent with the hypothesis that the functions of PPT1, TPP1 and CLN5 are nonredundant in the CNS, as has been suggested for TPP1 (43). Elucidation of the basic mechanisms that underlie the morphological changes by detailed analysis of the NCL animal models will be central to our future understanding of NCL pathogenesis.

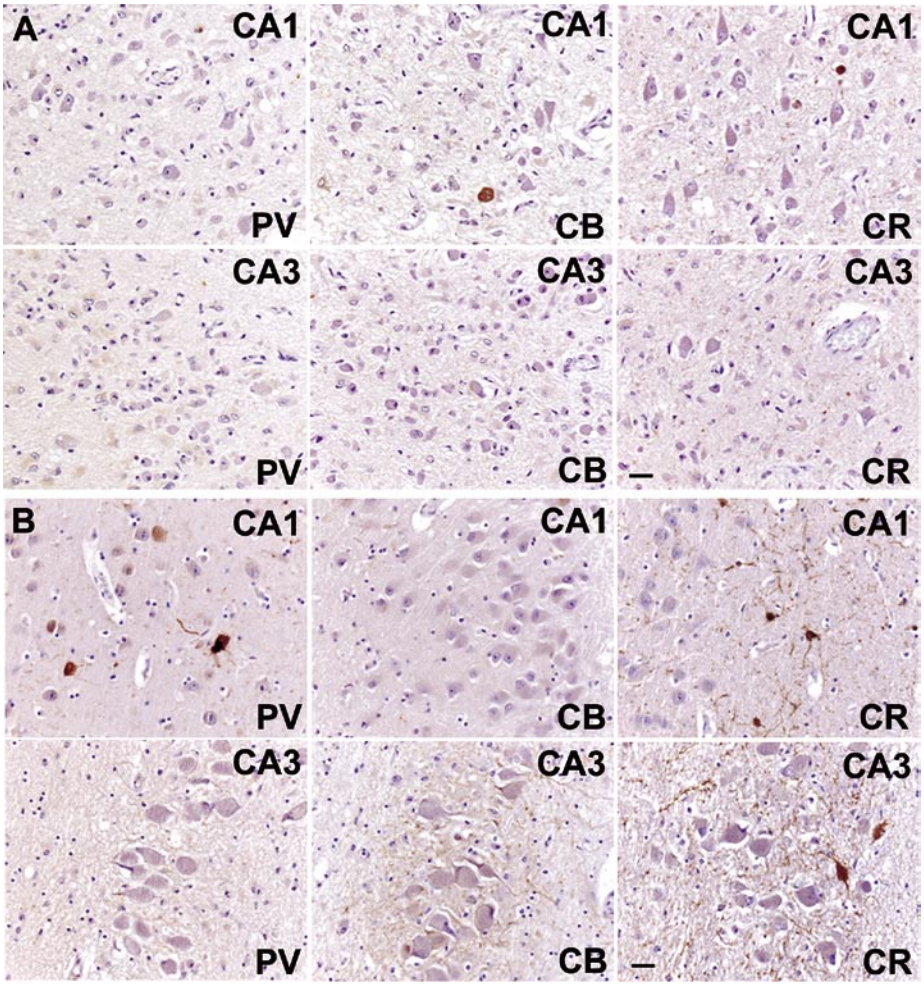

Figure 5. Loss of GABAergic interneurons in the NCL hippocampus. Immunohistochemical stainings for interneuron markers parvalbumin (PV), calbindin (CB), and calretinin (CR) demonstrated subfield- and phenotype-specific changes in interneuron survival. (A) In a pathologically less advanced CLN1 case, the loss of interneurons was complete within CA3, but occasional calbindin- and calretinin-positive interneurons remained amongst the persisting pyramidal neurons of CA1. (B) In CLN3, the relative preservation of parvalbumin- and calretinin-positive interneurons in CA1 compared with CA3 was evident. Calretinin-positive interneurons were best preserved across all hippocampal subfields and in all forms of NCL. Scale bar = 20 μm.

ACKNOWLEDGMENTS

We would like to thank colleagues in the Pediatric Storage Disorders Laboratory for their helpful discussions, Andrew Bylo for secretarial support, Mavis Kibble and Tuija Järvinen for expert technical assistance, Lauri Ylimaa for help in preparing the figures and Drs Payam Rezaie, Ming Lim, Alison Barnwell and Claire Russell for their constructive comments on this manuscript. This study was supported by grants from the Academy of Finland (207016, JT), Helsinki University Research Funds (2103029, JT), and from the US National Institutes of Health (NINDS) (NS041930, JDC), The Natalie Fund and The Batten

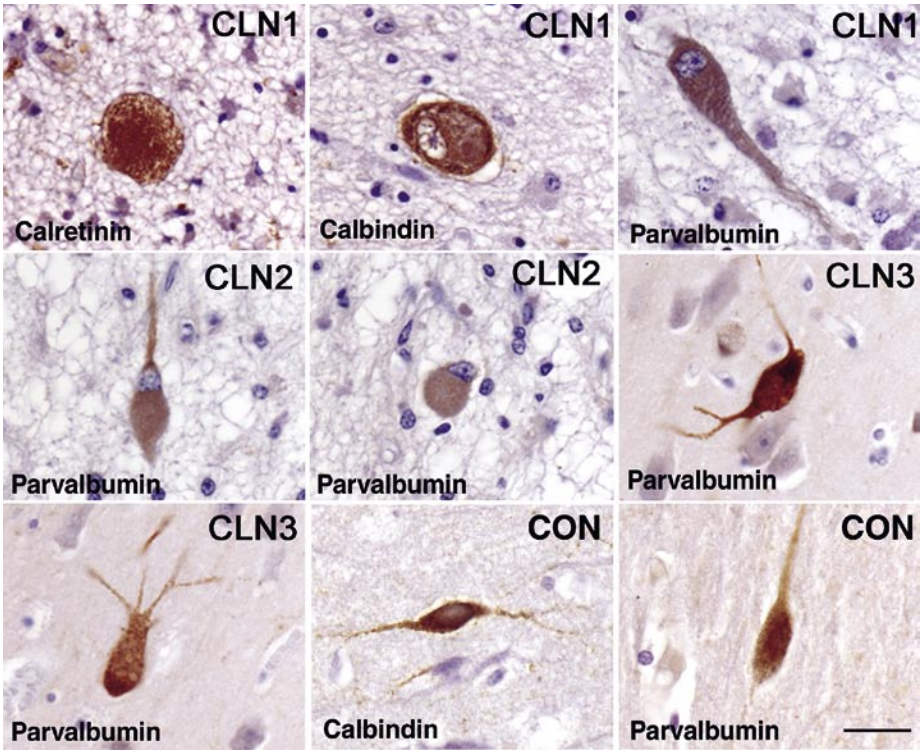

Figure 6. Pathological changes in the morphology of interneurons in NCL. In a pathologically less advanced case of CLN1 and in CLN2, the few surviving calretinin-, calbindin-, and parvalbumin-positive interneurons exhibited severe hypertrophy with pronounced ballooning of their soma. In CLN3 cases, interneuron loss was less pronounced, but the persisting interneurons displayed thickened and twisted dendritic morphology and prominent accumulation of storage material, compared to immunoreactive interneurons in control cases (CON). Scale bar = 20 μm.

Disease Family Association (JDC) and the Medical Research Council, United Kingdom (G9318379). Finally, we would like to acknowledge Prof Pirkko Santavuori (1933-2004), a dear colleague and friend, for her lifelong work on NCL-diseases, and dedicate this paper to her memory.

REFERENCES

1. Ahtiainen L, van Diggelen OP, Jalanko A, Kopra O (2003) Palmitoyl protein thioesterase is targeted to the axons in neurons. *J Comp Neurol* 455:368-377.

2. Bellizzi JJ III, Widom J, Kemp C, Lu JY, Das AK, Hofmann SL (2000) The crystal structure of palmitoyl-protein thioesterase 1 and the molecular basis of infantile neuronal-ceroid lipofuscinosis. *Proc Natl Acad Sci U S A* 97:4573-4578.

3. Bible E, Gupta P, Hofmann SL, Cooper JD (2004) Regional and cellular neuropathology in the palmitoyl protein thioesterase-1 (PPT1) null mutant mouse model of infantile neuronal ceroid lipofuscinosis. *Neurobiol Dis* 16:346-359.

4. Braak H, Goebel HH (1978) Loss of pigment-laden stellate cells: a severe alteration of the isocortex in juvenile neuronal ceroid-lipofuscinosis. *Acta Neuropathol* 42:53-57.

5. Braak H, Goebel, HH (1979) Pigmentoarchitectonic pathology of the isocortex in juvenile neuronal ceroid-lipofuscinosis: axonal enlargements in layer IIIab and cell loss in layer V. *Acta Neuropathol* 46:79-83.

6. Camp LA, Hofmann SL (1993) Purification and properties of a palmitoyl-protein thioesterase that cleaves palmitate from H-Ras. *J Biol Chem* 268:22566-22574.

7. Chattopadhyay S, Ito M, Cooper JD, Brooks AI, Curran TM, Powers JM, Pearce DA (2002) An autoantibody inhibitory to glutamic acid decarboxylase in the neurodegenerative disorder Batten disease. *Hum Mol Genet* 11:1421-1431.

8. Cooper JD, Messer A, Feng AK, Chua-Couzens J, Mobley WC (1999) Apparent loss and hypertrophy of interneurons in a mouse model of neuronal ceroid lipofuscinosis: evidence for partial response to insulin-like growth factor-1 treatment. *J Neurosci* 19:2556-2567.

9. Cooper JD (2003) Progress towards understanding the neurobiology of Batten disease or neuronal ceroid lipofuscinosis. *Curr Opin Neurol* 16:121-128.

10. Das AK, Lu J-Y, Hoffman SL (2001) Biochemical analysis of mutations in palmitoyl-protein thioesterase causing infantile and late-onset forms of neuronal ceroid lipofuscinosis. *Hum Mol Genet* 10:1431-1439.

11. De Lanerolle NC, Kim JH, Williamson A, Spencer SS, Zaveri HP, Eid T, Spencer DD (2003) A retrospective analysis of hippocampal pathology in human temporal lobe epilepsy: evidence for distinctive patient subcategories. *Epilepsia* 44:677-687.

12. D'Orlando C, Celio MR, Schwaller B (2002) Calretinin and calbindin D-28k, but not parvalbumin protect against glutamate-induced delayed excitotoxicity in transfected N18-RE 105 neuroblastoma-retina hybrid cells. *Brain Res* 94:181-190.

13. Freund TF, Buzsáki G (1996) Interneurons of the Hippocampus. *Hippocampus* 6:347-470.

14. Gao H, Boustany RM, Espinola JA, Cotman SL, Srinidhi L, Antonellis KA, Gillis T, Qin X, Liu S, Donahue LR, Bronson RT, Faust JR, Stout D, Haines JL, Lerner TJ, MacDonald ME (2002) Mutations in a novel CLN6-encoded transmembrane protein cause variant neuronal ceroid lipofuscinosis in man and mouse. *Am J Hum Genet* 70:324-335.

15. Goebel HH, Sharp JD (1998) The neuronal ceroid-lipofuscinoses. Recent advances. *Brain Pathol* 8:151-162.

16. Gupta P, Soyombo AA, Atashband A, Wisniewski KE, Shelton JM, Richardson JA, Hammer RE, Hofmann SL (2001) Disruption of PPT1 or PPT2 causes neuronal ceroid lipofuscinosis in knockout mice. *Proc Natl Acad Sci U S A* 98:13566-13571.

17. Haltia M, Rapola J, Santavuori P (1973a) Infantile type of so-called neuronal ceroid- lipofuscinosis. Histological and electron microscopic studies. *Acta Neuropathol (Berl)* 26:157-170.

18. Haltia M, Rapola J, Santavuori P, Keranen A (1973b) Infantile type of so-called neuronal ceroid-lipofuscinosis. 2. Morphological and biochemical studies. *J Neurol Sci* 18:269-285.

19. Haltia M (2003) The neuronal ceroid lipofuscinoses. *J Neuropathol Exp Neurol* 62:1-13.

20. Hofmann SL, Peltonen L (2001) The neuronal ceroid lipofuscinoses. In: *The Metabolic & Molecular Bases of Inherited Disease* (8th edition), Scriver CR, Beaudet AL, Sly WS, Valle D (Eds.) Vol III, pp 3877-3894, McGraw-Hill Companies Inc.

21. The International Batten Disease Consortium (1995) Isolation of a novel gene underlying Batten disease, CLN3. *Cell* 82:949-957.

22. Isosomppi J, Vesa J, Jalanko A, Peltonen L (2002) Lysosomal localization of the neuronal ceroid lipofuscinosis CLN5 protein. *Hum Mol Genet* 11:885-891.

23. Lehtovirta M, Kyttälä A, Eskelinen E-L, Hess M, Heinonen O, Jalanko A (2001) Palmitoyl-protein thioesterase localizes into synaptosomes and synaptic vesicles in neurons: implications for infantile neuronal-ceroid-lipofuscinosis (INCL). *Hum Mol Genet* 10:69-75.

24. Lonka L, Kyttälä A, Ranta S, Jalanko A, Lehesjoki A-E (2000) The neuronal ceroid-lipofuscinosis CLN8 membrane protein is a resident of the endoplasmic reticulum. *Hum Mol Genet* 11: 1691-1697.

25. Luiro K, Kopra O, Lehtovirta M, Jalanko A (2001) CLN3 is targeted to neuronal synapses but excluded from synaptic vesicles: new clues to Batten disease. *Hum Mol Genet* 10:2123-2131.

26. Mitchison HM, Bernard DJ, Greene NDE, Cooper JD, Junaid MA, Pullarkat RK, Vos N, Breuning MH, Owens JW, Mobley WC, Gardiner RM, Lake BD, Taschner PEM, Nussbaum RL (1999) Targeted Disruption of the Cln3 gene provides a mouse

model for Batten Disease. The Batten Mouse Model Consortium. *Neurobiol Dis* 6:321-334.

27. Mitchison HM, Lim MJ, Cooper JD (2004) Selectivity and Types of Cell Death in the Neuronal Ceroid Lipofuscinoses (NCLs). *Brain Pathol* 14: 86-96.

28. Mole SE (1999) Batten's disease: eight genes and still counting? *Lancet* 354:443-445.

29. Mole SE (2004) The Genetic Spectrum of Human Neuronal Ceroid-lipofuscinosis. *Brain Pathol* 14:70-76.

30. Oliet SH, Piet R, Poulain DA (2001) Control of glutamate clearance and synaptic efficacy by glial coverage of neurons. *Science* 292:923-926.

31. Oswald MJ, Kay GW, Palmer DN (2001) Changes in GABAergic neuron distribution in situ and in neuron cultures in ovine (OCL6) Batten disease. *Eur J Paediatr Neurol* 5 Suppl A:135-142.

32. Piet R, Poulain DA, Oliet SH (2002) Modulation of synaptic transmission by astrocytes in the rat supraoptic nucleus. J Physiol Paris 96:231-236.

33. Ranta S, Zhang Y, Ross B, Lonka L, Takkunen E, Messer A, Sharp J, Wheeler R, Kusumi K, Mole S, Liu W, Soares MB, Bonaldo MF, Hirvasniemi A, de la Chapelle A, Gilliam TC, Lehesjoki AE (1999) The neuronal ceroid lipofuscinoses in human EPMR and mnd mutant mice are associated with mutations in CLN8. *Nat Genet* 23:233-236.

34. Rezaie P, Male D (2002) Differentiation, ramification and distribution of microglia within the central nervous system examined. *Neuroembryology* 1:29-43

35. Salonen T, Heinonen-Kopra O, Vesa J, Jalanko A (2001) Neuronal Trafficking of palmitoyl protein thioesterase (PPT1) provides an excellent model to study the effects of different mutations which cause infantile neuronal ceroid lipofuscinosis (INCL). *Mol Cell Neurosci* 18:131-140.

36. Savukoski M, Klockars T, Holmberg V, Santavuori P, Lander ES, Peltonen L (1998) CLN5, a novel gene encoding a putative transmembrane protein mutated in Finnish variant late infantile neuronal ceroid lipofuscinosis. *Nat Genet* 19: 286-288.

37. Sleat DE, Donnelly RJ, Lackland H, Liu CG, Sohar I, Pullarkat RK, Lobel P (1997) Association of mutations in a lysosomal protein with classical late-infantile neuronal ceroid-lipofuscinosis. *Science* 277:1802-1805.

38. Suopanki J, Lintunen M, Lahtinen H, Haltia M, Panula P, Baumann M, Tyynelä J (2002) Status epilepticus induces changes in the expression and localization of endogenous palmitoyl-protein thioesterase 1. *Neurobiol Dis* 10:247-257.

39. Vesa J, Hellsten E, Verkruyse LA, Camp LA, Rapola J, Santavuori P, Hofmann SL, Peltonen L (1995) Mutations in the palmitoyl protein thioesterase gene causing infantile neuronal ceroid-lipofuscinosis. *Nature* 376:584-587.

40. Vesa J, Chin MH, Oelgeschläger K, Isosomppi J, Dell´Angelica EC, Jalanko A, Peltonen L (2002) Neuronal ceroid lipofuscinoses are connected at molecular level: Interaction of the CLN5 protein with CLN2 and CLN3. *Mol Biol Cell* 13:2410-2420.

41. Vines DJ, Warburton MJ (1999) Classical late infantile neuronal ceroid lipofuscinosis fibroblasts are deficient in lysosomal tripeptidyl peptidase I. *FEBS Lett* 443:131-135.

42. Warburton MJ, Bernardini F (2001) The specificity of lysosomal tripeptidyl peptidase-I determined by its action on angiotensin-II analogues. *FEBS Lett* 500:145-148.

43. Warburton MJ, Bernardini F (2002) Tripeptidyl peptidase-I is essential for the degradation of sulphated cholecystokinin-8 (CCK-8S) by mouse brain lysosomes. *Neurosci Lett* 331:99-102.

44. Wheeler RB, Sharp JD, Schultz RA, Joslin JM, Williams RE, Mole, SE (2002) The gene mutated in variant late-infantile neuronal ceroid lipofuscinosis (CLN6) and in nclf mutant mice encodes a novel predicted transmembrane protein. *Am J Hum Genet* 70:537-542.

45. Williams RS, Lott IT, Ferrante RJ, Caviness VS (1977) The cellular pathology of neuronal ceroid lipofuscinosis. *Arch Neurol* 34:298-305.